J Mater Sci (2009) 44:5441–5451
DOI 10.1007/s10853-009-3692-4

REVIEW

Negative thermal expansion: a review

W. Miller · C. W. Smith · D. S. Mackenzie · K. E. Evans

Received: 4 March 2009 / Accepted: 15 June 2009 / Published online: 2 July 2009

Abstract Most materials demonstrate an expansion upon heating, however a few are known to contract, i.e. exhibit a negative coefficient of thermal expansivity (NTE). This naturally occurring phenomenon has been shown to occur in a range of solids including complex metal oxides, polymers and zeolites, and opens the door to composites with a coefficient of thermal expansion (CTE) of zero. The state of the art in NTE solids is reviewed, and understanding of the driving mechanisms of the effect is considered along with experimental and theoretical evidence. The various categories of solids with NTE are explored, and experimental methods for their experimental characterisation and applications for such solids are proposed. An abstraction for an underlying mechanism for NTE at the supramolecular level and its applicability at the molecular level is discussed.

Introduction

In general, solids expand upon heating, i.e. they exhibit positive coefficients of thermal expansivity (CTE), denoted as α herein. However, a minority of solids show the inverse effect, i.e. of contracting upon heating, and thus exhibit negative thermal expansion (NTE). There has been an increasing amount of interest in these solids and their potential applications. The underlying mechanisms for NTE have been found to be complex.

W. Miller · C. W. Smith (✉) · D. S. Mackenzie · K. E. Evans
School of Engineering, Computing and Mathematics,
University of Exeter, Exeter EX4 4QF, UK
e-mail: c.w.smith@ex.ac.uk

The reason that most solids have positive CTEs is well understood which is due primarily to an increase in the interatomic bond length, which manifests at the macroscopic level as an overall increase in a dimension or volume. Bond lengthening is perhaps best explained by the potential energy versus interatomic distance diagram, see Fig. 1. On heating, the vibrational energy rises, and due to the asymmetry of the potential energy curve, shown in Fig. 1 (which can be considered typical of most strong bonds), the mean interatomic distance increases [1]. The rate of change (slope) of the potential energy curve is lower on the lengthening side of the curve than on the shortening side; thus, the mean bond length tends to increase with temperature. The so called 'stronger' bonds have steeper and narrower potential wells resulting in a slower rate of increase in interatomic distance, and hence a smaller thermal expansion coefficient (α). The CTE α is a measure of volumetric (α_v) or linear (α_l) change with temperature and is defined as

$$\alpha_V = \frac{\Delta V}{V_0 \Delta T} \tag{1}$$

$$\alpha_l = \frac{\Delta l}{l_0 \Delta T} \tag{2}$$

where ΔV, Δl are the changes in volume and length, respectively, V_0, l_0 are the initial volume and length, respectively, and ΔT is the change in temperature. In crystalline solids, α_V can be split to show the extent of expansion/contraction of individual crystal axial directions. In the case of isotropic solids, Eqs. 1 and 2 are related by $\alpha_v = 3\alpha_l$. However, in anisotropic solids, the relationship between α_l and α_V is not so simple as each crystal axis potentially has a different magnitude and sign of α giving three distinct values, α_a, α_b and α_c, contributing to α_V.

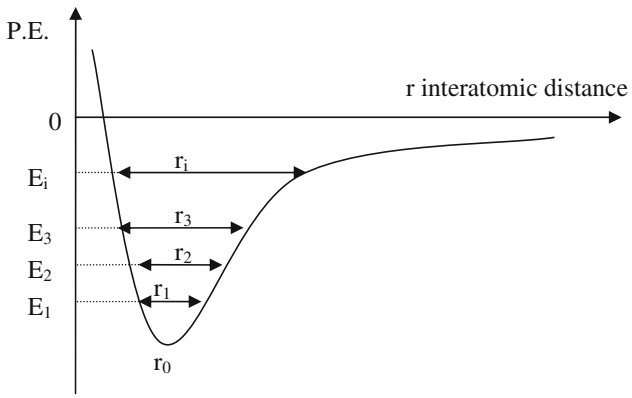

Fig. 1 Graph of a general anharmonic potential energy well, expanded for clarity, where E_i is the energy level and r_i is the interatomic distance

Several solids have now been identified with NTE behaviour, some associated with phase transitions and some stable over large temperature ranges. Examples include metal oxides [2–4], zeolites [5], AlpOs [6, 7], metal-organic frameworks [8] and other solids including well-known polymers [9–11] and fibres [12, 13]. The molecular and supramolecular structures of these solids are primary in determining whether the CTE is positive or negative [14].

Origin of negative thermal expansion

The NTE arises generally from supramolecular structural mechanisms, which dominate the erstwhile positive CTE of the interatomic bonds. No examples of solids with NTE in which the interatomic bond lengths shorten upon heating are known. In all the cases so far, the underlying mechanism for NTE is ascribed to higher order, i.e. supramolecular effects such as ferroelectric, magnetostrictive and displacive phase transitions, or low frequency phonon modes [15], the presence of rigid unit modes (RUMs) and libration. Ferroelectric phase transitions involve the ordering of dipole moments within a crystal structure. This occurs in BaT iO_3 when in the ferroelectric phase, due to slight distortions in the TiO_6 octahedra, the dipole moments are aligned (ordered) [16]. In the paraelectric phase (random), these dipoles are randomly orientated. Similarly, in transitions between ferro- and paramagnetic phases of a structure, the electron spins change, respectively, from being aligned to randomly orientated. Displacive phase transitions [16] occur frequently in metal oxide solids such as ZrV_2O_7 and quartz [17], whereby each atom in the crystal cell moves by a small amount relative to the surrounding atoms. These transitions do not involve any bond breaking or forming but can nevertheless significantly alter the structure between higher and lower symmetry forms. This is often manifested by rotations of rigid polyhedra units. However, the majority of structures found to exhibit NTE have a common feature which is the two-coordinate (planar) M–O–M or Si–O–Si linkage. These linkages are typical in metal oxides such as ZrW_2O_8-type solids and in zeolites, and are key to their NTE behaviour.

Bonds and associated vibrations

A phonon is a quantized mode of vibration, and may have a range of different frequencies, wavelengths and amplitudes, and be in or out of phase with each other. Two important phonon modes are the longitudinal and transverse vibrations depicted in Fig. 2. Upon heating the longitudinal vibration, modes tend to increase bond length, as explained above. In particular, M–O bonds increase in length which may, in turn, themselves promote an increase in M···M interatomic distances. In contrast, the transverse vibration modes can have an opposing effect on the M···M distance. This is sometimes given a 'guitar string' analogy, whereby, despite an increase in M–O bond length, the effective M···M distance decreases due to the change in M–O–M angle caused by the increase in amplitude of the oxygen atom's vibration. At this point, it is worth noting that transverse vibrational modes have lower excitation energy than longitudinal modes, and hence, they are excited at lower temperatures, which, in turn, means they more often dominate at lower temperatures. The response of the

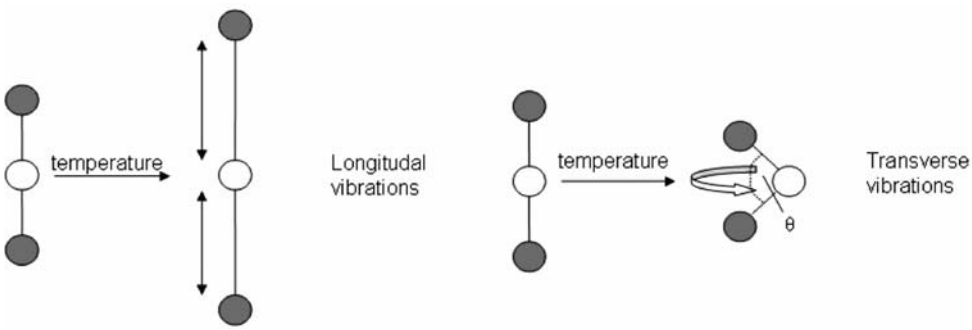

Fig. 2 Schematic showing on the *left*, longitudinal vibrations of M–O–M links found in network structures, and on the *right*, transverse vibrations responsible for NTE in some structures

M···M length is then a question of whether, in this case, the longitudinal or transversal modes dominate. It appears, in many open framework structures, that these modes are the origin of NTE at lower temperatures. The extent of this lower temperature range is determined by other factors. The phonons modes are related to α via the Grüneisen parameter γ [18]:

$$\alpha_V = \frac{\gamma C_V K}{V} \tag{3}$$

where C_v, K and V are the specific heat capacity, isothermal compressibility (also known as the bulk modulus), and volume, respectively. The Grüneisen parameter, γ, usually ascribed to a crystalline solid, reflects the anharmonicity of the various phonon modes present at a given temperature; negative values of which indicate that heating will produce a volumetric contraction, i.e. NTE, since all other parameters are constrained to be >0. The relationship of γ to particular phonon modes is

$$\gamma = \frac{-1}{2\omega^2}\frac{\delta\omega^2}{\delta s} \tag{4}$$

where ω is the frequency of the mode and s is an applied strain (zero in the case of a free standing solid). Phonon modes which show a decrease in frequency ω as volume decreases have a negative γ. Thus, a negative γ substituted into Eq. 3 gives an overall negative contribution to α, and hence a negative α [19]. Normal anharmonicity in simple atomic pair phonons as shown in Fig. 1 is reflected by a positive value for γ. More complex multi-atom phonons as shown in Fig. 2 may have negative values for γ.

Libration

There is a characteristic of variable temperature XRD that can show a perceived contraction in M–O bond lengths, when plotted against temperature. Classical asymmetric potential wells indicate that all the bonds expand with an increase in temperature, albeit at different rates due to the varying strengths of different bonds. A weaker bond will expand faster than a stronger bond. However, in diffraction experiments, a contraction in the Si–O bond length is often observed in silicates. This effect has been attributed to libration [19, 20]. Libration is a particular vibrational motion in a specific direction relative to the M–O bond. The XRD picks up an apparent shorter distance between M and O and, therefore, does not give the true bond length.

The librational effect is shown schematically in Fig. 3 [21]. If we consider the setup where two atoms A and B are bonded at a fixed length, R, lying along the x-axis, which denotes the mean orientation due to the mean positions of atoms hAi and hBi, then the bond librates about the Ox direction such that atoms A and B move as indicated in Fig. 3.

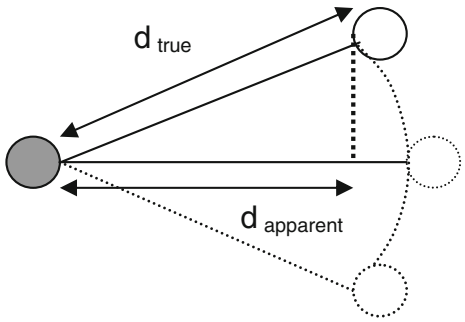

Fig. 3 Schematic showing the effect of libration of M–O links [21]

Furthermore, as the libration increases with temperature, the apparent bond length will decrease. It is worth noting at this stage that the apparent bond length will always be smaller than the true bond length. Furthermore, libration should not be confused with transverse vibrations, which although appear to be similar, are in fact different types of vibrations. However, it appears from current experimental data for zeolites that strong libration effects often accompany Si–Si contraction and transverse vibrations. In some cases, strong libration can show very negative apparent coefficients of thermal expansion αSi–O apparent, based on the change in apparent Si–O bond length with temperature.

Rigid unit modes

Structures consisting of corner-linked rigid polyhedra such as MO_4 are able to rotate about the so-called 'hinges', of the type M–O–M or M–O–M′ linkages, where M and M′ are metal cations. The polyhedra are much stiffer, i.e. have much higher frequency phonon modes, and so are relatively rigid in comparison with the M–O–M hinges which exhibit much lower frequency phonon modes. These modes are known as rigid unit modes (RUMs). In energy terms, the bending or rotation about the M–O–M linkage is many times more favourable than distortion of the polyhedral [22]. This is due to interatomic repulsions between electronegative oxygen atoms being very strong. The M–O–M hinges rotate due to the anharmonicity in their lateral vibrations as described by the Gruneisen parameter above.

The so-called quasi RUMS (QRUMs) are very similar to RUMs, but have merely low frequencies instead of near-zero frequencies. The effect of this is that the QRUMs have higher energy and unlike RUMs exhibit polyhedral rotations and slight distortions in some or all the rigid polyhedra. This was demonstrated in ZrV_2O_7 by Pryde et al. [23], where rotations of two-linked tetrahedral VO_4 caused small but significant distortions within the octahedral ZrO_6 units. Rigidity of polyhedra is mainly attributed to anion–anion

(oxygen–oxygen) repulsions. On increasing the cation size, the tetrahedra or octahedra increase in size, thus oxygen–oxygen distances increase resulting in a decrease in repulsion [24]. The reduced interaction strength in oxygen repulsions decreases the rigidity of the polyhedra allowing for distortions. The effect of this on NTE is shown in the $A_2M_3O_{12}$-type structure (M = W and A = most cations which can accept octahedral coordination), where increasing size of cation 'A' increased the effect of NTE [24, 25]. For rotations of the polyhedra in the $A_2M_3O_{12}$-type structure to occur, there must be slight distortions in the polyhedra. Thus, increasing cation size increases volume contraction. Rotations of polyhedra combined with polyhedral distortions are also seen in NASICON structures ($NaZr_2(PO_4)_3$). The QRUMs in the NASICON structure manifest themselves as rotations of rigid tetrahedra causing the octahedra to distort as the temperature is increased [26].

In a computational study by Hammonds et al. [27, 28], the phenomenon of local RUMs was discussed. Local RUMs were proposed as an integral part of structural flexibility, and are interesting in that they can result in localised thermally driven contraction of specific sections or cages within a framework structure. Local RUMs are essentially the same as RUMs, in that the rigid units rotate about M–O–M linkages thus causing a structural change. The main difference is that unlike RUMs, local RUMs are not present uniformly throughout the whole structure but are periodic. This phenomenon may have some special uses since local thermally driven contraction may alter local physico-chemical properties of these solids, e.g. catalytic activity. These local RUMs have been used to explain catalytic activity of certain zeolites, where non-framework molecules induce a change in the local structure [29].

Phase transitions

The RUMs cause changes in the M–O–M angles as explained above; however, some structures, despite possessing rigid polyhedra, do not show this cooperative rotation of linked polyhedra giving rise to NTE behaviour. This is due to the way in which they are arranged in the larger structural network. This can be seen in many structures which undergo a phase transition, at a particular temperature—a good example being the structure type $A_2(MoO_4)_3$ and the zeolite ferrierite [30]. It was shown [31] on a study of $Sc_2(MoO_4)_3$ that the monoclinic phase had a positive α_V, and the orthorhombic phase had a negative α_V. It was also shown [32] that generally such molybdate structures show positive α_V in the monoclinic phase; however, after a phase transition to an orthorhombic unit cell, α_V changes to negative. Symmetry is important in NTE and has been shown in many structures with displacive phase transitions, where a change in symmetry is accompanied by a change in the sign of α.

During phase transitions the RUMs act as 'soft modes' which have a low and strongly temperature-dependent frequency. Soft modes may also be described as 'particular excitation which becomes unstable as the system approaches, the stability limit' [33]. Whilst there is no specific limit to the number of 'soft modes', usually there is one particular mode responsible for the phase change. As the temperature approaches, the phase transition temperature, Tc, the 'soft mode' frequency approaches zero, and at Tc, the system is unstable and undergoes a phase change to a stable form. The displacive phase transition, e.g. from one ordered crystal structure to another, can be split into two types, namely first-order discontinuous (α/β-quartz transition) and second-order continuous (ferrierite [30] which changes symmetry from Pmmn to Immm) transitions. These transitions involve some change in symmetry, e.g. change in space group or crystal system [34], and may also involve a large reduction or increase in cell volume. However, in most first-order transitions there occurs a rapid increase in volume, which may subsequently be followed by contraction. A good example of this is the framework structure ZrV_2O_7. It was shown [35] that over the temperature ranging from −263 to 470 °C, there was a phase transition which corresponded to a change in α sign. It was suggested [23] that the existence of quasi-RUMs (QRUMs) was the reason for NTE in the high temperature phase. Phase transitions represent an interesting case of NTE, but given their very specific temperature dependencies, they do not have the wide range of applications of the more stable, wider temperature range NTE similar to other solids.

Microcracking

Anisotropic contraction can increase the apparent magnitude of reduction in volume of bulk samples when performing dilatometry measurements. This was reported on the metal oxide $Sc_2(WO_4)_3$ [36], where the ceramic bar showed an approximately fivefold increase in contraction compared to the powder ND-determined thermal expansion. The reason why this occurs is not fully understood; however, it is clear that some macroscopic mechanism combines with a molecular mechanism to enhance the NTE effect. This has been postulated as being primarily due to microcracking of a compacted bulk sample. However, recent study by the authors has suggested that mere structural disorder, as would be caused by microcracking, cannot by itself give rise to an NTE effect at the macroscopic size scale [37]. It is more likely that the compaction process gave rise to very specific packing and/or orientation of crystals and apparent amplification of an already anisotropic NTE in one axis with consequent diminution of NTE in the other axes. Notably, this effect is less likely to happen in cubic solids having isotropic NTE behaviour.

A generalised mechanism

A generalised mechanism for NTE can be demonstrated schematically using the simplified 2D diagram in Figs. 4 and 5, for the perovskite and zirconium tungstate solids, respectively. The generalised mechanism requires RUMs to be present, with suitably connected polyhedra and voids into which they are free to rotate. This depends upon the cooperative effects of the factors described in the sections above. In Fig. 4, the shaded squares show a slice through linked octahedra of MO_6 as seen in perovskite [38]. Figure 5 shows the *xy*-plane with rotations of linked octahedra about the *z*-axis. As can be clearly seen in both of these structures due to rotations of the octahedra, at the M–O–M angle, the unit cell (outlined in the figures) decreases in area, and voids between units alter significantly from squares to parallelograms. The angle θ (tilt angle) represents the degree of rotation/change in M–O–M angle. In 3D, this is repeated in the other planes resulting in a decrease in volume.

This cooperative rotation of rigid corner linked units also occurs in structures of linked tetrahedra [39] or a mixture of linked tetrahedra and octahedra [27, 31]. Rotation of the M–O–M angle is finite, in that there is a limit to the change in angle, due to intermolecular forces and interactions. This limit varies depending of type of polyhedra and the local constraint in effect for example different connectivity within the network structure. Consequently, issues such as framework connectivity can restrict and even prevent rotations of the linked polyhedra taking place. Lightfoot et al. [6] studied several zeolite structures, and found by comparison that many microporous zeolites show NTE, but despite similar structural units others do not, for example the PTE zeolite CIT-5 and $AlPO_4$-31. A framework structure or chiral symmetry possessing rigid units seems to be necessary but not sufficient for NTE behaviour to occur, as other as yet undefined structural conditions are equally necessary. The geometrical origin of NTE shown by Heine et al. [40], demonstrated some mathematical aspects of rotations of rigid units in framework structures. One particular finding not echoed by many other authors, was that polyhedral rotations occur throughout the phonon spectrum, and are not confined to low frequency modes. However, it was also pointed out that due to the harmonicity of the phonon modes as represented by γ is strongly dependent on ω (the phonon frequency, in fact ω^2), the lower phonon modes have a disproportionate effect. This was shown in the study on β-quartz [17].

Returning to the statement at the beginning of this section, when looking at NTE, there are essentially two mechanisms active during NTE. The thermal expansion between atom pairs has a positive contribution, whereas the geometric rotations of rigid units (transverse vibrational modes and libration) has a negative contribution. For NTE

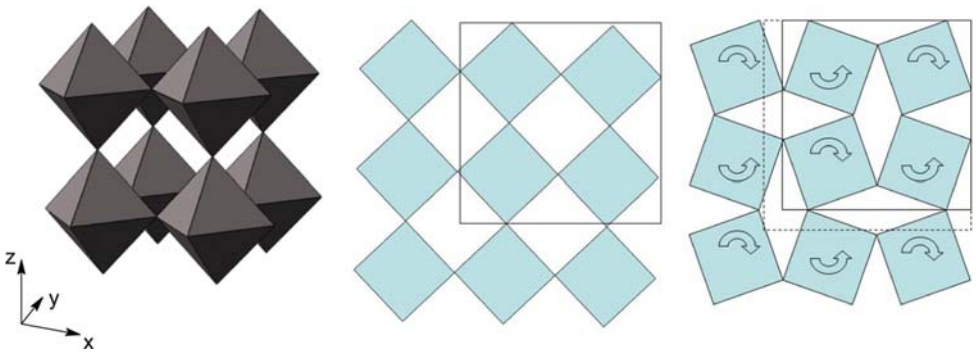

Fig. 4 Schematic of the perovskite structure shown as octahedral units and 2D representation shown as rotating squares, indicating the rotation mechanism

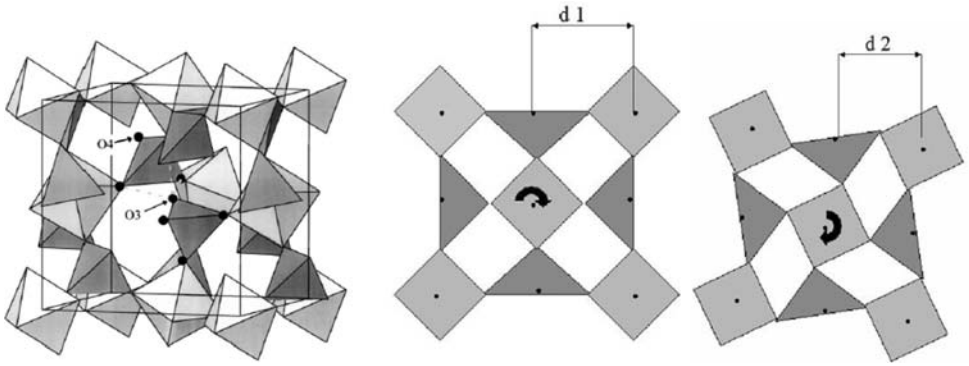

Fig. 5 Schematic of Zirconium Tungstate structure shown by tetrahedral and octahedral units in 3D [58] and the RUM mechanism in 2D

to occur then, the geometric effects (RUMs) must dominate those of the chemical bond expansion (longitudinal modes).

Framework flexibility

Structural flexibility is a key factor for NTE and a network structure requires a certain degree of flexibility for the rotations of polyhedra to occur. A crude, but useful method for determining potential structural flexibility was derived by J. C. Maxwell in 1864, which has been applied to different solids, for example on the stiffness of glass [41].

This method is ideal as an initial indicator of potentially flexible networks but is limited, and thus to determine the 'true' flexibility of network structures a more detailed analysis is required. This may be done computationally with emphasis on the various bond angles and symmetry of the structure. Two research groups in particular have looked at framework flexibility, using different approaches. Khosrovani and Sleight [42] studied several cubic network structures with emphasis on the role of symmetry in framework flexibility. They used structural refinements of different space groups on different network structures, allowing them to plot an agreement factor *R* against the unit cell parameter 'a'. It was shown that in some, but not all cases, a lowering of the space group resulted in an increase in lattice flexibility. In addition, lowering the space group appeared to have more pronounced effect on compressive rather than expansive flexibility, an example of which was zeolite rho, which subsequently showed to exhibit NTE [43]. This behaviour is more complex as it involves cation relocation in addition to rotations of rigid polyhedra. It is important to note that their analysis was based on linked polyhedra, and has been shown to be consistent with the RUM model. Hammonds et al. [27] approached the problem of structure flexibility by looking solely at the effect of RUMs on network flexibility with particular emphasis on local RUMs and provided good insight into their importance in framework flexibility.

Types of NTE materials

Framework or network structures encompass a large number of crystalline solids, ranging from zeolites to Aluminium phosphates ($AlPO_{4s}$), metal oxides to metallo-organic structures [44]. The common feature of these solids, aside from the metallo-organic structures, is the ability to break them down structurally into simple units made up of polyhedra. Depending on the presence of near-zero frequency phonon modes these polyhedra may or may not exhibit RUMs. Since the discovery of NTE, many different structures have been investigated, where CTEs have been predicted and experimentally measured. Noticeably, all these structures so far identified possess the M–O–M (or Si–O–Si) linkage. This study has been mainly carried out on framework type ceramics, for example ZrW_2O_8 and ZrV_2O_7, both of which have been extensively studied over their entire stability range and whose mechanisms are understood in detail. Study on NTE behaviour in zeolites has only just begun and little computational study or experimental measurements of α, have been made. There are several groups currently working on NTE behaviour in framework structures, Dove et al. [17, 27], have developed a computational program to investigate RUMs, whereas Woodcock and Lightfoot [45] have concentrated on zero expansion NASICON solids and some zeolites. Sleight et al. [46, 47] have mainly studied ZrW_2O_8 and related structures along with J. S. O. Evans and T. A. Mary who have also turned to $A_2(MoO_4)_3$ [31] and $A_2(WO_4)_3$ [36] type structures.

Zeolites

Zeolites are increasingly being studied by many research groups, in part, due to their wide range of applications. At present, there are approximately 150 different zeolite framework types, each of which has several elemental compositions. The diversity of zeolite structures is due to the multitude of ways in which the component tetrahedra can be linked [48], which, in turn, is due to the flexibility of the Si–O–Si linkages which can vary from 120° to 180°. The siliceous faujasite network structure is of particular interest as it has been shown to exhibit strong NTE behaviour [5, 6, 49–55]. The channels formed by joining sodalite cages in Faujasite network structures are dependent on connectivity and thus vary dramatically in size from very small in zeolite A, to very large in zeolite VPI-5. The directions of these sodalite cage channels depend on the crystal symmetry and tend to run along crystal lattice directions. When NTE occurs, these cages and channels effectively fold in on themselves due to the rotations of tetrahedra. It was shown [56, 57] via simulation that zeolites with only 1D channels running through them tend not to show NTE behaviour, where as zeolites with 2D or 3D channels do. It was concluded that thermal expansion behaviour is, in part, dependent on the type of sodalite cage channel system.

Metal oxides

AM_2O_8-type structures

Other framework structures of particular interest are those of the ZrW_2O_8 family (AM_2O_8, where 'A' = any cation capable of octahedral coordination and M = W or Mo), which have been the subject of much investigation due to

their strong NTE properties. Similar to zeolites, their framework not only comprises tetrahedral units but also includes octahedral units, which are arranged as corner sharing polyhedra with all the six oxygen atoms on the ZrO_6 being shared with WO_4 tetrahedra, Fig. 1.10a [58]. The WO_4 tetrahedra have one terminal oxygen which is important in the phase transition at approximately 450 K. These tetrahedra are aligned along the body diagonal [1 1 1], with the terminal oxygen atoms pointing along the diagonal. During the phase transition, these oxygen atoms change orientation and react with their nearest neighbour tetrahedra, resulting in oxygen migration [19]. The consequence of the free terminal oxygen is the unusual effect in the solid state of increasing the degree of freedom. With the 'active' RUMs in ZrW_2O_8 under heating, and due to ZrW_2O_8 having a cubic crystal structure, the interesting phenomenon of isotropic contraction occurs. This reduces the likelihood of microcracking and is of particular interest for use in composites [59]. If the 2D perovskite type rotating squares mechanism is considered for ZrW_2O_8, then rotating squares are interlinked by triangles, causing area and volume contraction as shown by Fig. 5. ZrW_2O_8 has an average linear coefficient of negative thermal expansion of $\alpha_l = -9.07 \times 10^{-6}\ K^{-1}$ [4, 18, 19] over the temperature range of $T = 0$–350 K, which represents a degree of contraction comparable to the degree of positive thermal expansion seen in most solids. Interestingly, ZrW_2O_8 is one of the few structures that exhibits NTE over its entire stability range. In comparison, cubic $ZrMo_2O_8$ has a lower average linear $\alpha_l = -6.9 \times 10^{-6}\ K^{-1}$ and $\alpha_l = -5.0 \times 10^{-6}\ K^{-1}$ (below and above the phase transition, respectively) over the temperature ranges 2–200 K and 250–502 K [60]. This reduction in NTE effect is due to the presence of the smaller Mo cation in comparison to W.

Zirconium Vanadate ZrV_2O_7

Zirconium Vanadate, ZrV_2O_7, is structurally related to ZrW_2O_8, where two WO_4 tetrahedra are replaced by V_2O_7 (M_2O_7) itself comprising two corner-linked VO_4 tetrahedra. This changes the crystallographic symmetry, but the overall cubic crystal structure and an isotropic NTE behaviour are retained. In the average unit cell, four of the six crystallographically unique V_2O_7 have, according to the symmetry, linear V–O–V linkages, which at high temperatures bend away from 180° and pull the structure in on itself. It is suggested that this is a high energy form and that, in reality, any two linked VO_4 tetrahedra rotate relative to one another to reduce the angle [23]. However, it has been shown that no RUMs exist in ZrV_2O_7, but instead QRUMs, where coupled rotations of the VO_4 tetrahedra are accompanied by slight distortions of the ZrO_6 octahedra, resulting in a balance between the stiffness of ZrO_6 and the energy gain from V–O–V bending [24]. The NTE effect is smaller, if the tetrahedra are smaller, and in the case of ZrP_2O_7, α is positive. Unlike ZrW_2O_8, ZrV_2O_7 has a phase change which changes α from low-temperature expansion to high-temperature contraction.

$A_2W_3O_{12}$

The $A_2W_3O_{12}$-type structure is particularly interesting as it clearly demonstrates the effect of changing cation size on NTE behaviour. As with most metal oxides, the only constraints on cation 'A' is that it must be able to adopt the octahedral coordination and be trivalent, for example Al, Sc, Y, Lu, Ho. The $A_2W_3O_{12}$ structure is formed by corner-linked AO_6 and WO_4 polyhedra, forming M–O–M and A–O–M linkages. It was suggested [24] that in the $Sc_2W_3O_{12}$ structure rocking of the polyhedra could only occur if slight changes, e.g. distortions, took place in the polyhedra. Hence, it was implied that the rigidity of polyhedra inhibits NTE. Rigidity of the polyhedra is an effect of anion–anion repulsion, in this case O–O repulsions, which are stronger in smaller polyhedra as the oxygen atoms are closer together. Thus, by increasing polyhedral size, replacing Sc with a larger cation, will increase their ability to deform, and hence, to increase the NTE effect. This was confirmed [24] by experimental results on $Lu_2W_3O_{12}$ which had a considerably stronger contraction, $\alpha = -6.8 \times 10^{-6}\ K^{-1}$, as opposed to $Sc_2W_3O_{12}$ $\alpha = -2.2 \times 10^{-6}\ K^{-1}$. This cation size effect was confirmed [25] by an experimental study on $A_2W_3O_{12}$, $Sc_2W_3O_{12}$ and $Y_2W_3O_{12}$, where a clear progression from increasing cation size caused greater thermal contraction. They also showed that this trend correlates to changes in M–O_6–W_2 angle, which expands the most as temperature increases, where the smaller the cation the smaller this angle, thus allowing for greater opening of this angle as temperature rises.

$A_2M_4O_{15}$ and $AOMO_4$

The structures $A_2M_4O_{15}$ and $AOMO_4$ are similar to the other metal oxides described before, having corner linked octahedra and tetrahedra, by A–O–M and M–O–M linkages. A study on $Ln_2Mo_4O_{15}$ (Ln = Y, Dy, Ho, Tm) [61] suggested that NTE occurred over a large temperature range, and was shown to have structural elements similar to ZrW_2O_8 and ZrV_2O_7, e.g. MoO_4 and Mo_2O_7 units. $Dy_2Mo_4O_{15}$ showed no large change in α over the temperature range from 30 to 200 °C, and suggests that no first-order phase transition occurs in this range. However, it was suggested that a second-order phase transition as seen in ZrW_2O_8 may occur. The negative thermal expansion in

these structures is not as large as that seen in ZrW_2O_8 and $Sc_2W_3O_{12}$, and there is no evidence of increasing cation size increasing the NTE effect, in fact the opposite occurs. These structures and $AOMO_4$ have not been studied much, and more detailed analysis is needed to understand their NTE behaviour. $AOMO_4$ structures show anisotropic negative thermal expansion above a phase transition at 200 °C and anisotropic positive expansion below, which has been attributed to rocking of the rigid polyhedra about weak A–O–M linkages [62, 63].

AlPOs

$AlPO_4$ structures are very similar to those of zeolites and have been shown experimentally and by predictive methods to have either PTE or NTE behaviour [6, 7]. However, in either case, the thermal expansion behaviour is shown to be anisotropic in nature. $AlPO_4$-5 is a typical example made up of four and six membered rings, such as those found in zeolites, which combine to form large twelve membered channels running along the z-axis of the structure. There are two different types of tetrahedra those of AlO_4 and PO_4, where the AlO_4 tetrahedra are larger than the PO_4 tetrahedra [64]. As in zeolites, rotations about Al–O–P angles result in a collapse of the channels and NTE.

NASICON

The NASICON structure is based on $NaZr_2(PO_4)_3$, and is of interest due to its approximately zero thermal expansion. NASICON structures possess anisotropic CTE, with expansion in two axial directions but a decrease in the third. The general structure of $NaTi_2(PO_4)_3$ [65] is a 3D lattice of vertex-linked TiO_6 octahedra and PO_4 tetrahedra. In the complex thermal expansion of NASICON structures, the CTE behaviour is governed by different factors in each variant, for example $LiTi_2(PO_4)_3$ shows a migration of the Li cation from MI to MII sites [45], whereas in $Sr0.5Ti_2(PO_4)_3$, it is due to the combining effects of polyhedra rotating and vacant sites.

Carbon nanotubes

Recently [66–69], it has been found that carbon nanotubes may exhibit negative thermal expansion over certain temperature ranges. Although the magnitude of the coefficients of thermal expansion in carbon nanotubes are not as great as in zeolites and metal oxides, they are still a significant effect. The NTE mechanism is not fully understood; therefore, it may be a perceived effect and not a true thermal contraction as seen in zeolites and metal oxides.

Metal organic frameworks (MOFs)

Recent studies [8, 70] have identified the new class of nanoporous solids called metal organic frameworks (MOFs) which can exhibit very large negative (but highly anisotropic) thermal expansion, of a magnitude significantly greater than that for metal oxides and zeolites. These MOFs consist of rigid polyhedra connected by relatively under-constrained linkers to form large cavities. Anisotropy in the thermal expansion of the crystal structure drives a structural reorganisation resulting in the collapse of the cavities in a similar manner to that described by Miller et al. [37]. The MOFs studied showed that these structures have strong volumetric NTE which becomes larger as the length of linker is increased. These structures are promising candidates for applications in catalysis, storage/release and separations, due to their large tailorable voids and NTE, linked with good stability.

Applications

Owing to their complex but flexible structures zeolites have a very wide range of applications in many different industries. Zeolites have been in use primarily in the petroleum industry for many years now and are a fundamental aspect of petroleum cracking. Their selective catalytic activity is what makes them useful in the cracking process. They are, however, used at high temperature, and thus, knowledge of how they react to such temperatures is vital to optimising the process. Many of the zeolites studied so far show NTE behaviour, and being stable at high temperature means they are particularly interesting for the petroleum cracking industry. However, detailed studies of the effect of NTE on catalytic activity are lacking, and require a detailed understanding of NTE mechanisms in zeolites. Their catalytic properties are also vital for various high temperature commercial chemical reaction processes.

Zeolites, zeolite-like solids and metal oxides with NTE are also of interest in composites particularly in the microchip industry [47, 71]. Thermal expansion behaviour of dental fillings has been studied, with the intention of finding a better match between the thermal expansion of tooth and filling under conditions of rapid changes in temperature [72]. This is where composites of positive and negative α solids would be of great use. They also have a similar potential application as fillers in adhesives, where warming of the adhesive can result in expansion and weakening of the bond between components. Composites with a particular α value may be tailored by including a NTE solid in the composite, thus reducing thermal stresses and weakening bonds as temperature rises. Essentially this approach simply transfers the problem of a CTE

mismatch-driven stress at the interface between two monolithic materials, to that of a stress within a composite adhesive layer. Whilst it is usually preferable to avoid stresses at interfaces, one must consider the issue of stresses acting at particle–matrix interfaces within the composite adhesive layer. However, good particle–matrix interface strengths are achievable [59]. It was shown [73] how composites made from negative and positive α components can be successfully tailored to give approximately zero thermal expansion of the bulk composite. Zeolites with NTE behaviour have applications in aerospace technologies [74], in electronics [47], as well as in fibre optics [75], fuel cells and high precision optical mirrors [47].

Experimental measurements of α

The most common methods of obtaining experimental measurements of α are temperature varying X-ray or neutron diffraction. X-ray (XRD) and Neutron diffraction (ND) patterns can be determined using powder (PXRD) or single crystal samples and offer a precise method for determining crystal structures [45, 76]. XRD and ND measurements can be recorded at varying temperatures and is above all non-destructive, though diffraction data does not always correspond to the bulk thermal expansion. From these patterns, all the cell parameters are easily determined, and the effect of changing temperature on them is used to calculate the linear and volume coefficients of thermal expansion. Dilatometry is used to measure α of bulk solid samples such as ceramic block, or large single crystals and involves heating the sample in a furnace where the resulting expansion or contraction is measured by being mechanically transmitted via 'push rods' to displacement sensors. The disadvantages of this method are that only one axis at a time is measured, and the accuracy is dependent on the expansion of the push rods, which are made of different solids depending on the temperature range of the measurements, e.g. fused silica for up to 700 °C, Alumina up to 1600 °C and for higher temperatures graphite. Dilatometry measurements tend to give smaller α values, as seen in $Sc_2W_3O_{12}$ [36, 77], which has been attributed to microcracks in the ceramic blocks or large crystals; however, the exact mechanisms are not fully understood.

Design of supramolecular NTE structures

There have been several studies of design NTE structures [78–86] at the supramolecular size scale; perhaps, one could consider this as going beyond the realm of chemistry into that of materials science or engineering. The mechanisms used in the design of Supramolecular structures are, by definition, structural and therefore are not bounded in the same way that materials properties might be, as shown by Rosen and Hashin [87]. Therefore it is possible to design structures with extremal thermal properties without sacrificing other important considerations, such as stiffness. These studies can be broadly divided into two mechanisms: those which use positive thermal expansion of one material to generate a Poisson's ratio contraction in another; those which use thermal expansion in one solid to drive angle changes of internal structures to effect NTE, in a similar manner to the mechanism for NTE materials. Both approaches assume small (linear) deformation theory throughout. The former category consists of studies by Landert and Ito [78, 79] who developed composite fibre shearing mechanisms, Lim [80] who proposed a re-entrant structure similar to structures used to give a negative Poisson's ratio and Kelly [81, 82] who proposed a direct competition between thermal expansion and transverse strain. The latter category contains studies by Aboudi and Qi [83, 84], Sigmund and Torquato [85] and Lakes [86] who proposed multi-solid structures where differing thermal expansivities of components drive rotating, hinging or flexing beams. All of these present specific examples of structures with NTE behaviour, but until recently what was missing was a generalised set of underlying principles for CTE in such supramolecular structures, providing a framework for rational design of NTE or indeed extreme positive CTE structures. Miller et al. [37] provided such an underlying framework that can be shown to fully describe the specific NTE mechanisms in all of the previous studies. The mechanism of Miller et al. is based on a simple triangular unit cell with beams of dissimilar CTE. The beams are treated as such in this article and have the specific constitutive properties associated with pin-jointed beams as could be found in truss structures, but in fact they could be generalised to any type of interaction such as flexing beams, phases in a fibrous or particulate composite, or even interatomic potentials. Within a specified range of geometries and constitutive material properties (primarily CTEs), an increase in temperature drives an internal angle change that dominates the inherent positive CTE of the constituent materials and engenders the unit cell with an overall NTE. This effect is unbounded (positive or negative) and may be achieved using conventional, i.e. positive CTE, constituent materials. A range of unit cells are available built from triangular subunits, providing anisotropic or isotropic extreme CTEs in 2D or 3D, or even the biomaterial strip of Lakes [86] (the internal angles are simply set to 180° and 0°). Given the constraints of the simplified interaction potentials used in this approach, it may still be possible to design extreme CTEs at the molecular scale, if the triangular mechanism is not dominated by the

more complex range of interactions in operation at that size scale.

Conclusions

Interest in negative thermal expansion materials has increased greatly in the last decade, stemming from and prompting further discovery of many new NTE materials. This has especially concerned improved understanding of the underlying atomistic and molecular mechanisms, as well as the identification of a raft of new potential applications. Of all of these applications, probably the most developed is the use of NTE fillers to modify the overall CTE of particulate composites, especially for use in microchip packaging. The key patent in this area proposes the use of zirconium tungstate to reduce the CTE of microchip underfill adhesive [88], which will lead to increased operating temperatures or increased fatigue life [59].

Understanding of NTE materials increases the possibilities for new synthetic and more extreme NTE materials improve, such as MOFs [8, 70]. Those materials will undoubtedly have applications in their own right as sensors etc., as well as fillers in composites. Given the current scientific interest in NTE and its potential for practical application, there will be no doubt many further discoveries concerning NTE. A more generalised understanding of NTE in such solids has been attempted [71], and the importance of rigid and relatively much more flexible structural units or linkages is evident, but the question remains as to why some solids posses NTE, and apparently structurally similar compatriots do not. From an engineering or materials point of view, there are several interesting future directions in which NTE materials may go. One such direction not yet exploited at all concerns the tuned CTE components, which exactly counter-match thermal expansion of components with differing thermal expansivity. Truss-type structures with tuned expansivity [78–86] may offer reductions in distortion for dimension-critical components such as those used for telecommunications and scientific equipment. Since density is a function of CTE and temperature, composite or monolithic materials with tuned CTE would throw up the possibility of manipulation of many other density-dependent properties. These would include elastic wave speed and hence acoustic refractive index, and electromagnetic properties such as resistivity and optical refractive index.

Of all the NTE materials, perhaps, the most promising are the MOFs with their relatively much larger NTEs. Their NTEs seem to be large enough to make polymer matrix composites with near-zero CTE using practically realisable filler volume fractions via standard manufacturing routes. Such large NTEs also promise use in MEMS and NEMS where they could function as thermally driven actuators, or compensators for CTE mismatch, although their other mechanical properties make them less attractive as engineering materials. Supramolecular truss-type structures, at first, seem applicable only at the gross macro scale, since their manufacture seems to require large-scale joining process. However, recent advances in manufacturing processes such as rapid prototyping/manufacturing are reducing the size scale at which they can function, the range of usable materials, and most importantly unit cost. A relatively cheap additive process with sub-millimetre resolution does not seem too far away, and would throw up the possibility of truss-type micro structures, with bespoke CTE, in a net-shape manufacturing process. Component redundancy and weight reduction arising from compounding multiple functionalities into single materials ought to reduce total energy cost of manufacture, which becomes especially important in transport applications, energy cost in service etc.

References

1. Chang R (2000) Physical chemistry for the chemical and biological sciences, 3rd edn. University Science Books, Sausalito
2. Evans JSO, David WIF, Sleight AW (1999) Acta Crystallogr B 55:333
3. Evans JSO, Hu Z, Jorgensen JD, Argyriou DN, Short S, Sleight AW (1997) Science 275:61
4. Mary TA, Evans JSO, Vogt T, Sleight AW (1996) Science 272:90
5. Attfield MP, Sleight AW (1998) Chem Mater 10:2013
6. Lightfoot P, Woodcock DA, Maple MJ, Villaescusa LA, Wright PA (2001) J Mater Chem 11:212
7. Tao JZ, Sleight AW (2003) J Phys Chem Solids 64:1473
8. Goodwin AL, Calleja M, Conterio MJ, Dove MT, Evans JSO, Keen DA, Peters L, Tucker MG (2008) Science 319:794
9. Baughman RH, Turi EA (1973) J Polym Sci B 11(12):2453
10. Baughman RH (1973) J Chem Phys 58(7):2976
11. Baughman RH, Galvado DS (1995) Chem Phys Lett 240(1–3): 180
12. Rupnowski P, Gentz M, Sutter JK, Kumosa M (2005) Compos Part A 36:327
13. Yamanaka A, Kashima T, Tsutsumi M (2007) J Compos Mater 41(2):165
14. Sleight AW (1995) Endeavor 19(2):64
15. Ernst C, Broholm G, Kowach R, Ramirez AP (1998) Nature 396(12):147
16. Dove MT (1997) Am Miner 82:215
17. Welche PRL, Heine V, Dove MT (1998) Phys Chem Miner 26:63
18. Evans JSO, David WIF, Sleight AW (1999) Acta Crystallogr B 55:333
19. Evans JSO (1999) J Chem Soc Dalton Trans 331:7
20. Mittal R, Chaplot SL (2000) Solid State Commun 115:319
21. Barrera GD, Bruno JAO, Barron THK, Allan NL (2005) J Phys Condens Matter 17:217
22. Hammonds KD, Bosenick A, Dove MT, Heine V (1998) Am Miner 83:476
23. Pryde AKA, Hammonds KD, Dove MT, Heine V, Gale JD, Warren MC (1996) J Phys Condens Matter 8:10973

24. Forster PM, Yokochi A, Sleight AW (1998) J Solid State Chem 140:157
25. Woodcock DA, Lightfoot P, Ritter C (2000) J Solid State Chem 149:92
26. Woodcock DA, Lightfoot P, Smith RI (1999) J Mater Chem 9:2631
27. Hammonds KD, Heine V, Dove M (1998) J Phys Chem B 102:1759
28. Hammonds KD, Deng H, Heine V, Dove MT (1997) Phys Rev Lett 78(19):3701
29. Sanchez-Vallea C, Sinogeikin SV, Lethbridge ZAD, Walton RI, Smith CW, Evans KE, Bass JD (2005) J Appl Phys 98:053508
30. Bull I, Lightfoot P, Villaescusa LA, Bull LM, Glover RKB, Evans JSO, Morris RE (2003) J Am Chem Soc 125:4342
31. Evans JSO, Mary TA (2000) Int J Inorg Mater 2:143
32. Tyagi AK, Achary SN, Mathews MD (2002) J Alloys Compd 339:207
33. Schneider T, Srinivasam G, Enz C (1972) Phys Rev A 5(3):476
34. Cochran W (1973) The dynamics of atoms in crystals. Edward Arnolds, London
35. Khosrovani N, Sleight AW (1997) J Solid State Chem 132:355
36. Evans JSO, Mary TA, Sleight AW (1998) J Solid State Chem 137:148
37. Miller W, Mackenzie DS, Smith CW, Evans KE (2008) Mech Mater 40:351
38. Giddy P, Dove MT, Pawley GS, Heine V (1993) Acta Crystallogr A 49:697
39. Woodcock DA, Lightfoot P, Villaescusa LA, Diaz-Cabanas MJ, Camblor MA (1999) J Mater Chem 9:349
40. Heine V, Welche PRL, Dove MT (1999) J Am Ceram Soc 82(7):1793
41. Phillips JC (1979) J Non-Cryst Solids 34:153
42. Khosrovani N, Sleight AW (1996) J Solid State Synth 121:2
43. Reisner BA, Lee Y, Hanson JC, Jones GA, Parise JB, Corbin DR, Toby BH, Freitag A, Larese JZ, Kahlenberg V (2000) Chem Commun 222:1
44. Wu Y, Kobayashi A, Halder G, Peterson V, Chapman K (2008) Angew Chem Int Ed 47:8929
45. Woodcock DA, Lightfoot P (1999) J Mater Chem 9:2907
46. Kameswari U, Sleight AW, Evans JSO (2000) Int J Inorg Mater 2:333
47. Closmann C, Sleight AW (1998) J Solid State Chem 139:424
48. Weller MT (2001) Inorganic materials chemistry: Oxford chemistry primers. Oxford University Press, Oxford University
49. Martinez-Inesta MM, Lobo RF (2005) J Phys Chem B 109(19): 9389
50. Johnson MR, Kearley GJ, Buttner HG (1999) AIP Conf Proc 479:28
51. Reisner BA, Lee Y, Hanson JC, Jones GA, Parise JB, Corbin DR, Toby BH, Freitag A, Larese JZ, Kahlenberg V (2000) Chem Commun 22:2221
52. Marinkovic BA, Jardim PM, Saavedra A, Lau LY, Baehtz C, de Avillez RR, Rizzo F (2004) Micropor Mesopor Mater 71(1):117
53. Jardim PM, Marinkovic BA, Saavedra A, Lau LY, Baehtz C, Rizzo F (2004) Micropor Mesopor Mater 76(1):23
54. Sen S, Wusirika RR, Youngman RE (2006) Micropor Mesopor Mater 87:217
55. Yamahara K, Okazaki K, Kawamura K (1995) Catal Today 23:397
56. Tschaufeser P, Parker SC (1995) J Phys Chem 99(26):10609
57. Bieniok A, Hammonds KD (1998) Micropor Mesopor Mater 25(1):193
58. Ramirez AP, Kowach GR (1998) Phys Rev Lett 80(22):4903
59. Miller W, Smith CW, Burgess AN, Dooling PJ, Evans KE (2008) Phys Status Solidi B 245(3):552
60. Allen S, Evans JSO (2003) Phys Rev B 68:134101
61. Sebastian L, Sumithra S, Manimama J, Umarji AM, Gopalakrishnan J (2003) Mater Sci Eng B103:289
62. Amos TG, Yokochi A, Sleight AW (1998) J Solid State Chem 14:303
63. Sleight AW (1998) Inorg Chem 37:2854
64. Liu Y, Withers RL, Noren L (2003) Solid State Sci 5:427
65. Woodcock DA, Lightfoot P, Ritter C (1998) Chem Commun 1:107
66. Maniwa Y, Fujiwara R, Kira H, Tou H, Kataura H, Suzuki S, Achiba Y, Nishibori E, Takata M, Sakata M, Fujiwara A, Suematsu H (2001) Phys Rev B 64:241402
67. Tomanek D (2005) J Phys Condens Matter 17:R413
68. Kwon YK, Berber S, Tomanek D (2004) Phys Rev Lett 92(1):015901
69. Brown S, Cao J, Musfeldt JL, Dragoe N, Cimpoesu F, Ito S, Takagi H, Cross RJ (2006) Phys Rev B 73:125446
70. Dubbeldam D, Walton KS, Ellis DE, Snurr RQ (2007) Angew Chem Int Ed 46(24):4496
71. Sleight AW (1998) Curr Opin Solid State Mater Sci 3:128
72. Versulius A, Douglas WH, Sakaguchi RL (1996) Dent Mater 12:290
73. Tran KD, Groshens TJ, Nelson JG (2001) Mater Sci Eng A303:234
74. Imanaka N, Hiraiwa M, Adachi G, Dabkowska H, Dabkowski A (2000) J Cryst Growth 220:176
75. Clegg JW, Kelly A (2002) Adv Eng Mater 4(6):388
76. Couves JW, Jones RH, Parker SC, Tschaufeser P, Catlow CRA (1993) J Phys Condens Matter 5:L329
77. Evans JSO, Mary TA, Sleight AW (1997) J Solid State Chem 133:580
78. Landert M, Kelly A, Stearn RJ (2004) J Mater Sci 39:3563. doi:10.1023/B:JMSC.0000030707.91634.5f
79. Ito T, Suganuma T, Wakashima K (1999) J Mater Sci Lett 18:1363
80. Lim T (2005) J Mater Sci 40:3275. doi:10.1007/s10853-005-2700-6
81. Kelly A, McCartney LN, Clegg WJ, Stearn RJ (2005) Compos Sci Technol 65:47
82. Kelly A, Stearn RJ, McCartney LN (2006) Compos Sci Technol 66:154
83. Aboudi J, Gilat R (2005) Int J Solids Struct 42:4372
84. Qi J, Halloran JW (2004) J Mater Sci 39:4113. doi:10.1023/B:JMSC.0000033391.65327.9d
85. Sigmund O, Torquato S (1996) Appl Phys Lett 69:21
86. Lakes R (1996) J Mater Sci Lett 15:475
87. Rosen BW, Hashin Z (1970) Int J Eng Sci 8:157
88. Shih-Fang C, McKinney TX (2005) Low coefficient of thermal expansion semiconductor packaging materials. US Patent US2005/0110168 A1